# 3-D Simulation and Visualization of Laminar Flow in a Microchannel with Hair-Pin Curves

**Y. Yamaguchi, F. Takagi, K. Yamashita, H. Nakamura, and H. Maeda**
National Institute of Advanced Industrial Science and Technology, Tosu 841-0052, Japan

**K. Sotowa and K. Kusakabe**
Dept. of Applied Chemistry, Kyushu University, Fukuoka 812-8581, Japan

**Y. Yamasaki and S. Morooka**
Dept. of Chemical Engineering, Fukuoka University, Fukuoka 814-0180, Japan

*The purpose of the present study was to investigate fluidic behavior in a microchannel with hair-pin curves, using a three-dimensional (3-D) computational fluid dynamics simulation, and to observe the 3-D flow pattern, to validate the simulation. The microchannel used was fabricated on a PMMA plate using a flat-end mill. The channel width and depth were 210 and 205 μm, respectively, and the radius of each hair-pin curve was 500 μm. Two liquids; purified water and an aqueous solution of 50 μmol/L fluorescein, were introduced into the microchannel through different inlets and were merged, forming a side-by-side parallel flow in the straight channel. When the average velocity was 25 mm/s, the liquid was thrust outward by centrifugal force and, as a result, the vertical line that crossed the central axis was distorted after passing the first hair-pin curve. At the second hair-pin curve, the centrifugal force was exerted in the opposite direction, and the distorted line returned nearly to an initial vertical line. When the average velocity was 125 mm/s, however, the vertical line, which was distorted at the first hair-pin curve, did not recover to the initial vertical line after the second curve. The interface between the two liquids was permanently waved. The simulation was in good agreement with the experimental data. The results suggest that the diffusion rate through the interface of two liquids in microchannels with hair-pin curves can increase, compared to that in straight microchannels. © 2004 American Institute of Chemical Engineers AIChE J, 50: 1530–1535, 2004*
*Keywords: microfluidics, confocal fluorescence microscopy, computational fluid dynamics, microchannel, microreactor*

## Introduction

Miniaturized devices for use in chemical analysis and material synthesis have attracted considerable interest in recent years (Ehrfeld, 2000). These devices usually contain microchannels, the widths of which are 1–1000 μm. Such narrow channels provide unique reaction fields, basically because the outside surface area per unit reactor volume is large in comparison with conventional reactors. Examples of such applications include: the selective synthesis of organic compounds using organic and aqueous phases (Hisamoto et al., 2001), the enzyme reaction with

---

Correspondence concerning this article should be addressed to H. Maeda at maeda-h@aist.go.jp.
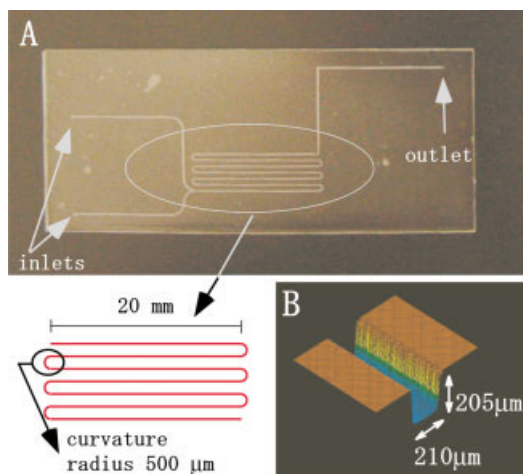
**Figure 1. Fabrication of a microchannel. A: top view, B: details of the channel.**

high yields (Kanno et al., 2001; Miyazaki et al., 2001), and the synthesis of nanoparticles with well-controlled sizes (Nakamura et al., 2002). When particles that are lighter or heavier than the liquid are suspended in a microchannel with sharp corners, a centrifugal force is induced. As a result, the path lines of the particles deviate from the path lines of the liquid stream. The same effect would be expected when two liquids with different densities are introduced into microchannels.

For liquid-phase systems in microchannels, the diffusion rate is a key factor in controlling reaction rates. Because the flow is laminar, the diffusion rate between the two liquids is dependent on the contact area. We recently reported on some two-dimensional (2-D) observations of flow characteristics in a microchannel (width = 210 $\mu$m, depth = 205 $\mu$m) with hair-pin corners (Kawazumi et al., 2002). Red- and green-colored water with the same density were introduced into the microchannel in a side-by-side parallel flow mode, and the flow pattern was observed from the vertical direction using a color CCD camera with a 200× magnifying lens. The color of the microchannel flow changed before and after the hair-pin corner. This was caused by a local circulating flow, induced by a centrifugal force acting on the homogeneous liquid. The interface area and, as a result, the diffusion between the two liquids could be influenced by this secondary flow. However, the flow was observed only from the vertical direction, and we were not able to elucidate the three-dimensional (3-D) behavior of the liquids.

The purpose of the present study is to demonstrate microfluidic behavior using 3-D computational fluid dynamics simulation, and to validate the simulation by observing the 3-D hydrodynamic behavior. At the macro level, fluidic simulation and visualization have been extensively performed, and the secondary flow induced at a corner has been analyzed (Cheng et al., 1976; Ghia and Sokhey, 1977). At the micro level, however, research on 3-D flow visualization has been only recently begun. Wang et al. (1995) used small beads as the tracer, but these beads might disturb the flow in a microspace. Manz et al. (1995) measured the

velocity distribution in a capillary using an NMR micro-imaging technique, but the spatial resolution was larger than 10 $\mu$m, which was not sufficiently small for measurements in microchannels. In contrast, a measurement technique using single-molecule fluorescein, coupled with fluorescence confocal microscopy, was recently developed and permitted a description of flow with a spatial resolution as small as 1 $\mu$m (Gösch et al., 2000; Ismagilov et al., 2000). We directed our attention to applying this principle to observations of the cross-sectional plane of fluids in microchannels and to clarify the interface configuration. An understanding of the flow dynamics would be highly desirable for designing chemical reactions at the interface of solutions (Kenis et al., 1999; Zhao et al., 2002), as well as extraction between aqueous and organic phases (Hisamoto et al., 2001), and, furthermore, in elucidating the origin of much higher chemical reaction yields in microchannel reactors, compared to those in well-mixed batch reactors (Kanno et al., 2001; Miyazaki et al., 2001; Tanaka et al., 2001).

## Experimental Studies

A microchannel was fabricated mechanically on a PMMA plate (Kawazumi et al., 2002), using a Robodrill (FANUC, Oshino-mura, Japan) with a flat-end mill (diameter = 200 $\mu$m, Hitachi Power Tools, Osaka, Japan). Figure 1a shows a complete view of the microchannel used, and Figure 1b shows the details of the channel. The channel width and depth were 210 and 205 $\mu$m, respectively. The radius of each hair-pin curve was 500 $\mu$m, unless otherwise stated. The wall roughness was determined to be less than 5% of the depth, as evidenced by a laser microscope measurement. After fabrication, the channel plate was covered with a plat top plate and sealed by heating. Programmable syringe pumps were connected to the inlets by Teflon tubing.

Two liquids were prepared: purified water and an aqueous solution of 50 $\mu$mol/L fluorescein. The densities were practically the same. The two liquids were introduced into the microchannel through different inlets and were merged to form a side-by-side parallel flow in the straight channel. A confocal fluorescence microscopy system (Nikon, Tokyo,
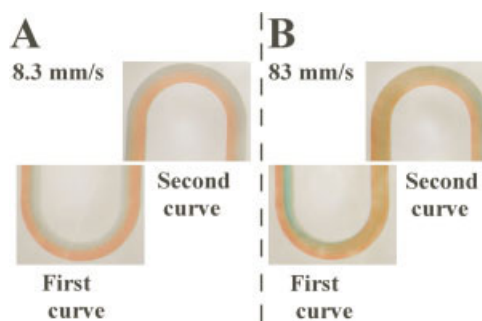


**Figure 2. Two-dimensional observation of flow using red- and green-colored water. Two liquids are introduced into the channel in a side-by-side parallel flow configuration.**
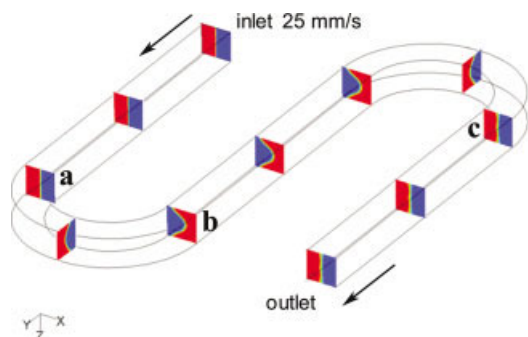
**Figure 3. Distortion of the initially vertical line during its passage through the microchannel (simulation). Average velocity = 25 mm/s.**
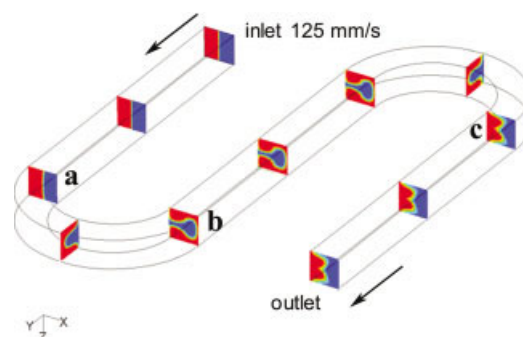


**Figure 5. Distortion of the initially vertical line during its passage through the microchannel (simulation). Average velocity = 125 mm/s.**

Japan) was used for the measurement. An Ar laser (wavelength = 488 nm, output = 25 mW) was scanned through an objective lens (ELWD-20x) in a 3-D manner, and the fluorescence emission from the fluorescein solution was detected at a resolution of about 3 $\mu$m. To observe the 2-D flow pattern, samples of red- and green-colored water were also used. The color change in the microchannel flow was recorded through the upper cover plate.

## Computational Fluid Dynamics Simulation

The dimensions of the microchannel used for the simulation are assumed to be: width = depth = 200 $\mu$m, straight channel length = 20 mm, and curvature radius = 500 $\mu$m. Three-dimensional simulations were carried out using FLUENT 6.0 (Fluent USA, Lebanon, NH) based on a finite-volume scheme. The Euler mixing model, suitable for mutually miscible fluids, was adopted. Molecules of the liquid microscopically slip on the channel wall (Thompson and Trolan, 1997). For simplicity, however, no slip conditions were assumed in the present study (Barrat and Bocquet, 1999; Stroock et al., 2002). The inlet plane was divided in 40 × 40 mesh sections, and the total number of mesh

sections in the calculated space was 475,200. A computation with nearly double the number of mesh sections gave approximately the same results. An iterative calculation for solving the Navier–Stokes equations was carried out with the second-order accuracy for pressure, and the SIMPLE algorithm was used for pressure–velocity coupling.

## Results and Discussion

Figure 2 shows a 2-D observation of the flow pattern, using the red- and green-colored waters. When the average velocity is 8.3 mm/s, the two liquids form a side-by-side parallel flow, and no color change is observed in the microchannel. When the average flow velocity is increased to 83 mm/s, however, the outside red region overrides the inside green region after the first hair-pin curve, and the color of the flow changes to red. After passing the second turn with an opposite curvature, a green liquid emerges, and the flow pattern returns to the original side-by-side parallel flow.
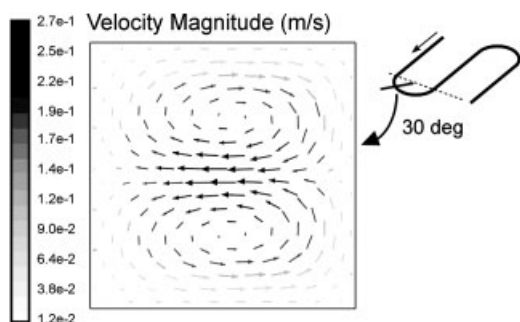
Figure 3 shows the result of the simulation at an average velocity of 25 mm/s. The velocity along the central axis is
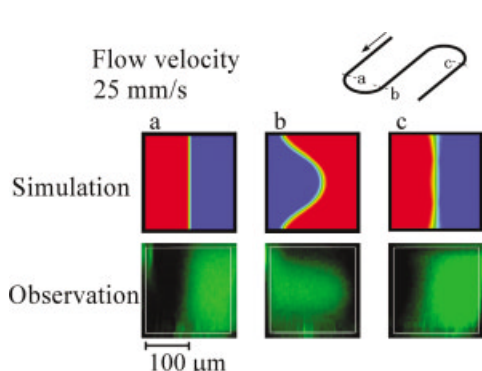


**Figure 4. Comparison between simulation and experiment for 3-D flow patterns. Average velocity = 25 mm/s.**
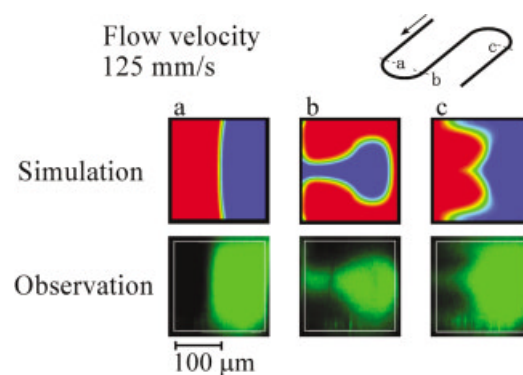


**Figure 6. Comparison between simulation and experiment for 3-D flow patterns. Average velocity = 125 mm/s.**

**Figure 7. Velocity distribution of the secondary flow at the first turn. Average velocity = 125 mm/s.**

the largest and is the most strongly affected by the centrifugal force. As a result, the liquid flowing along the central axis is thrust outward the most vigorously. Thus, the vertical line that crosses the central axis is distorted after the first-turn. After the second turn, the centrifugal force is exerted in the opposite direction, and the distorted line returns nearly to the initial vertical line.

Figure 4 shows a comparison between the simulation and the experimental results for the vertical cross-sectional plane under the same conditions as were used in Figure 3. The average liquid velocity is 25 mm/s. The upper and lower pictures a, b, and c correspond to the situations before the first turn, after the first turn, and after the second turn, respectively. The lines in the upper pictures, calculated by the simulation, indicate a boundary between the water and the fluorescein solution. The fluorescein solution, which initially flows on the right-hand side in this cross section, is thrust outward after the first turn and then returns to the initial position after the second turn. The simulation is in good agreement with the experimental data.

Figure 5 shows the results of the simulation and an observation for the case where the average velocity is 125 mm/s. The vertical line observed in the initial straight channel is heavily distorted after the first turn. After the second turn, the two liquid flows largely return to the original positions, and the side-by-side parallel flow pattern is again observed. In contrast with the result for a velocity of 25 mm/s, however, the distorted line is not fully recovered to the initial vertical line after the second turn. The interface between the two liquids is permanently distorted by the stronger centrifugal force. Figure 6 shows a comparison between simulation and observation at a velocity of 125 mm/s. The upper pictures show the calculated interfaces, and the lower pictures show the results of the 3-D observation. The upper and lower pictures agree well, as was found for a velocity of 25 mm/s.

Figure 7 shows the velocity distribution on the vertical plane perpendicular to the main liquid flow at the middle point of the first turn. The liquid at the outer periphery is forced outward, and the liquid at the upper and lower periphery moves inward to compensate for the outward flow. This secondary flow perturbs the interface configuration. These results are in agreement with findings for laminar flow

at the macro level (Cheng et al., 1976; Ghia and Sokhey, 1977). The flow in a curved channel is expressed by the Dean number

$$k = \text{Re} \sqrt{a/R} \qquad (1)$$

where Re is the Reynolds number, $a$ is the channel radius, and $R$ is the curvature radius. A single vortex pair appears in the region of $K < 140$ (Ghia and Sokhey, 1977). The value of the Dean number in the present study is less than 20, which supports the formation of secondary flows in the microchannel.

Liquid-phase chemical reactions and material syntheses in 3-D microspaces are substantially influenced by diffusion across the interface. The degree of diffusion is expressed by the parameter $P_Z$

$$P_Z = \frac{Dt}{L^2} \qquad (2)$$

where $D$ is the diffusion coefficient, $t$ is the time of diffusion, and $L$ is the representative length of the space. The representative length can be defined by

$$L = 6V/S \qquad (3)$$

where $V$ is the volume and $S$ the interfacial area through which diffusion occurs (Crank, 1975). In a microchannel with hair-pin curves, the interface of the two liquids is not a simple flat plane, as seen in Figures 4 and 6. Figure 8 summarizes the interface configurations as functions of average velocity and curvature radius. Data for hair-pin curves with a curvature radius of 250 $\mu$m are included in this figure. The interfacial area per unit length of the microchannel increases to $\alpha S_0$, where $S_0$ is the flat interfacial area and $\alpha$ ($=S/S_0$) is a coefficient larger than unity. Parameter $P_Z$ is inversely proportional to $L^2$, indicating that the time required for diffusion decreases with an increase in $(\alpha S_0)^2$. As shown in Figure 8, $\alpha$ exceeds 3 in some cases. This suggests that the diffusion rate through the interface of the two liquids in microchannels with hair-pin curves greatly increases in comparison with that in straight microchannels. Because the two liquids used in this study are miscible, the interface of the liquids disappears after passing a certain number of hair-pin curves. In some cases, reaction rates may be strongly affected by the manner in which aqueous solutions are fed and mixed in microchannels (Kanno et al., 2001; Miyazaki et al., 2001; Tanaka et al., 2001). A further study of the role of microchannel curvature is currently under way.

| Flow velocity (mm/s) / Curvature radius (μm) | 25 $\alpha$ ($S/S_0$) | 75 $\alpha$ | 125 $\alpha$ |
|---|---|---|---|
| after first curve 500 | 1.5 | 2.5 | 3.5 |
| after first curve 250 | 1.5 | 2.4 | 3.2 |
| after second curve 500 | 1.0 | 1.3 | 1.8 |
| after second curve 250 | 1.0 | 1.5 | 2.3 |

**Figure 8. Effects of curvature diameter and average velocity on flow patterns and interface configurations in the microchannel.**

## Conclusions

Three-dimensional computational fluid dynamics simulations were performed, with respect to the fluidic behavior of laminar liquid flows in microchannels with hair-pin curves. The simulation results were validated by 3-D observation by confocal fluorescence microscopy. These results revealed that the interface configuration of two liquids was affected by secondary flow, induced by centrifugal force at the corners. The increased interface area of two laminar liquids could promote a mass transfer based on diffusion. The success of chemical reactions and material syntheses inside microchannels is often dependent on flow properties, and higher yields are obtained, compared to reactions in well-mixed reactors. The results obtained in this study suggest the importance of microchannel design based on a 3-D comprehension of the fluid and accompanying mixing behavior.

## Acknowledgments

## Literature Cited

Barrat, J.-L., and L. Bocquet, "Influence of Wetting Properties on Hydrodynamic Boundary Conditions at a Fluid/Solid Interface," *Faraday Discuss.*, **112**, 119 (1999).

Cheng, K. C., R.-C. Lin, and J.-W. Ou, "Fully Developed Laminar Flow in Curved Rectangular Channels," *Trans ASME: Ser. I*, **98**(1), 41 (1976).

Crank, J., *The Mathematics of Diffusion*, 2nd ed., Clarendon Press, Oxford, UK (1975).

Ehrfeld, W., *Microreaction Technology: Industrial Prospects*, Springer-Verlag, Berlin (2000).

Ghia, K. N., and J. S. Sokhey, "Laminar Incompressible Viscous Flow in Curved Ducts of Regular Cross Sections," *Trans. ASME: Ser. I*, **99**(4), 640 (1977).

Gösch, M., H. Blom, J. Holm, T. Heino, and R. Rigler, "Hydrodynamic Flow Profiling in Microchannel Structures by Single Molecule Fluorescence Correlation Spectroscopy," *Anal. Chem.*, **72**(14), 3260 (2000).

Hisamoto, H., T. Saito, M. Tokeshi, A. Hibara, and T. Kitamori, "Fast and High Conversion Phase-Transfer Synthesis Exploiting the Liquid–Liquid Interface Formed in a Microchannel Chip," *Chem. Commun.,* **24**, 2662 (2001).

Ismagilov, R. F., A. D. Stroock, P. J. A. Kenis, G. Whitesides, and H. A. Stone, "Experimental and Theoretical Scaling Laws for Transverse Diffusive Broadening in Two-Phase Laminar Flows in Microchannels," *Appl. Phys. Lett.*, **76**(17), 2376 (2000).

Kanno, K., H. Maeda, S. Izumo, M. Ikuno, K. Takeshita, A. Tashiro, and M. Fujii, "Rapid Enzymatic Transglycosylation and Oligosaccharide Synthesis in a Microchip Reactor," *Lab on a Chip*, **2**(1), 15 (2002).

Kawazumi, H., A. Tashiro, K. Ogino, and H. Maeda, "Observation of Fluidic Behavior in a Polymethylmethacrylate-Fabricated Microchannel by a Simple Spectroscopic Analysis," *Lab on a Chip*, **2**(1), 8 (2002).

Kenis, P. J. A., R. F. Ismagilov, and G. M. Whitesides, "Microfabrication Inside Capillaries Using Multiphase Laminar Flow Patterning," *Science*, **285**(5424), 83 (1999).

Manz, B., P. Stilbs, B. Jönsson, O. Söderman, and P. T. Callaghan, "NMR Imaging of the Time Evolution of Electroosmotic Flow in a Capillary," *J. Phys. Chem.*, **99**(29), 11297 (1995).

Miyazaki, M., H. Nakamura, and H. Maeda, "Improved Yield of Enzyme Reaction in Microchannel Reactor," *Chem. Lett.*, **5**, 442 (2001).

Nakamura, H., Y. Yamaguchi, M. Miyazaki, M. Uehara, H. Maeda, and P. Mulvaney, "Continuous Preparation of CdSe Nanocrystals by a Microreactor," *Chem. Lett.*, **10**, 1072 (2002).

Stroock, A. D., S. K. Dertinger, G. M. Whitesides, and A. Ajdari, "Patterning Flows Using Grooved Surfaces," *Anal. Chem.*, **74**(20), 5306 (2002).

Tanaka, Y., M. N. Slyadnev, K. Sato, M. Tokeshi, H.-B. Kim, and T. Kitamori, "Acceleration of an Enzymatic Reaction in a Microchip," *Anal. Sci.*, **17**(7), 809 (2001).

Thompson, P. A., and S. M. Troian, "A General Boundary Condition for Liquid Flow at Solid Surfaces," *Letters to Nature*, **389**(6649), 360 (1997).

Wang, W., Y. Liu, G. J. Sonek, M. W. Berns, and R. A. Keller, "Optical Trapping and Fluorescence Detection in Laminar Flow Streams," *Appl. Phys. Lett.*, **67**(8), 1057 (1995).

Zhao, B., N. O. L. Viernes, J. S. Moore, and D. J. Beebe, "Control and Applications of Immiscible Liquids in Microchannels," *J. Am. Chem. Soc.*, **124**(19), 5284 (2002).